sustainability

MDPI

Article

Removal of Azo Dyes from Water on a Large Scale Using a Low-Cost and Eco-Friendly Adsorbent

Ma. Guadalupe Aranda-Figueroa [1], Rosenberg J. Romero [2], Mario Rodríguez [3], Adriana Rodríguez-Torres [4], Alexis Rodríguez [5], Gloria Ivette Bolio-López [6], Dulce María Arias-Ataide [7], Álvaro Torres-Islas [1] and Maria Guadalupe Valladares-Cisneros [1,*]

1 Faculty of Chemical Sciences and Engineering, Autonomous University of the State of Morelos, University Ave. 1001, Chamilpa, Cuernavaca 62209, Morelos, Mexico; ma.arandafgr@fcqei.uaem.edu.mx (M.G.A.-F.); alvaro.torres@uaem.mx (Á.T.-I.)
2 Center for Research in Engineering and Applied Sciences, Autonomous University of the State of Morelos, University Ave. 1001, Chamilpa, Cuernavaca 62209, Morelos, Mexico; rosenberg@uaem.mx
3 Centro de Investigaciones en Óptica, A. P. 1-948, Lomas del Campestre, León 37000, Guanajuato, Mexico; mrodri@cio.mx
4 Department of Aeronautical Engineering, Polytechnic Metropolitan University of Hidalgo, Tolcayuca 1009 Ex Hacienda San Javier, Tolcayuca 43860, Hidalgo, Mexico; adrodriguez@upmh.edu.mx
5 Center of Research in Biotechnology, Autonomous University of the State of Morelos, University Ave. 1001, Chamilpa, Cuernavaca 622092, Morelos, Mexico; alexis.rodriguez@uaem.mx
6 Basic Science and Engineering, Popular University of La Chontalpa, Carretera Cardenas-Huimanguillo km 2.0, Cardenas 86500, Tabasco, Mexico; gloria.bolio@upch.mx
7 Higher Education School from Jicarero, Autonomous University of the State of Morelos, Carretera Galeana-Tequesquitengo s/n, Jojutla 62915, Morelos, Mexico; dulce@uaem.mx
* Correspondence: mg.valladares@uaem.mx

Abstract: The use of natural materials as adsorbents and the environmentally friendly removal of pollutants and azo dyes from water are important topics today. The goal of this research work was to assess the utility of *Luffa cylindrica* (*L. cylindrica*) as a natural and non-conventional adsorbent for azo dyes in water on a large scale (2 L). An azo dye (AD) at a concentration of 0.250 g/L was removed from the solution at a rate of 63.07% using 10.0 g/L doses of *L. cylindrica*, and the maximum adsorption capacity of *L. cylindrica* was 25.25 mg/g. *L. cylindrica* desorbed 95.8% of the AD in 0.1 M NaOH. Thermodynamically, the adsorption occurs through pseudo-second-order kinetics and the behaviors adjust better to the Langmuir isotherm. The analysis of variance (p-value < 0.05) shows that the contact time and the concentration of AD significantly influence the adsorption capacity and removal of AD. Few studies have examined the environmentally friendly removal of azo dyes from water using a natural non-conventional adsorbent.

Keywords: *Luffa cylindrica*; environmentally friendly removal of pollutants; adsorption

Academic Editors: Iuliana Deleanu and Cristina Busuioc

Received: 13 April 2025
Revised: 9 May 2025
Accepted: 12 May 2025
Published: 23 May 2025

Citation: Aranda-Figueroa, M.G.; Romero, R.J.; Rodríguez, M.; Rodríguez-Torres, A.; Rodríguez, A.; Bolio-López, G.I.; Arias-Ataide, D.M.; Torres-Islas, Á.; Valladares-Cisneros, M.G. Removal of Azo Dyes From Water on a Large Scale Using a Low-Cost and Eco-Friendly Adsorbent. *Sustainability* **2025**, *17*, 4816. https://doi.org/10.3390/su17114816

1. Introduction

The pollution level observed in water today is alarming. The sixth Agenda 2030 Sustainable Development Goal is to "ensure availability and sustainable management of water and sanitation for all". In order to achieve this goal, there is a need to study and apply environmentally friendly alternative technologies to remove pollutants from water. Recently, it was mentioned that environmental pollution is the principal cause of illness and premature death, especially in infants [1]. The low quality of wastewater produces many changes in ecosystems and human health [2,3].

Likewise, anthropogenic activities produce a wide variety of pollutants, such as drugs, solid wastes, microplastics, metals, and dyes, among others. Many of these pollutants

are discharged into the sewer system, runoff, and rivers and reach bodies of water [3,4]. Industries are the principal source of pollutants. The oil and textile industries play an important role in producing high volumes of toxic effluents. For instance, the textile industry uses more than 10,000 tons of dyes annually [5,6].

Synthetic dyes are widely used because they provide clothing with bright and attractive colors. However, many are resistant to light, detergents, and some chemical products. Currently, more than 3000 different dyes can be classified according to their chromophore group—for example, azo (-N=N-), nitro (O–N=O), and carbonyl (>C=O), among others [5,7]. Many others have more than one azo group in their chemical structure. Around the world, azo dyes represent more than 70% of the synthetic dyes used [8]. In addition, the presence of amines and benzene rings reduces their degradability and increases their toxicity and genotoxicity. Moreover, the widespread disposal of synthetic dyes in water increases the risks to human health [6,9].

Wastewater with dye concentrations below 0.100 g/L shows high values regarding the biological oxygen demand (BOD), chemical oxygen demand (COD), total suspended solids (TSS), and alkalinity [10]. The upper limits on the permitted levels of dyes in wastewater depend on the current standards of different cities and countries. However, the dye concentration reported in wastewater ranges from 55.8 to 1680 μg/L [11].

Chemical processes, such as the Fenton reaction, ozonation, and electrocoagulation, are used to produce colorless wastewater, but they generate high volumes of slurry, which is frequently more toxic than their initial pollutants, requiring subsequent treatments for its reduction [12]. The efficacy of biologically coupled processes for wastewater treatment depends on reducing the dye concentration before introducing wastewater into the bioreactors. Good and efficient pre-treatment ensures adequate biological cleaning processes because the high carbon charge produces a loss of the biofilms and the system efficiency reduces or changes. Some authors suggest that adsorption is a good coupling technique as a pre-treatment in wastewater biotreatment to reduce BOD and COD and eliminate TSS [13–15].

Adsorption is an efficient, easy, and promising process widely employed in engineering and cleaning up water [16]. Conventional adsorbents (Figure 1), such as active carbon and clays, are used in wastewater treatments.

However, adsorbents from natural sources are limited and expensive [13,17]. Therefore, non-conventional adsorbents from biomass, agro-industrial residues, and plants are proposed as friendly, low-cost, and sustainable alternatives for treating wastewater [18,19].

An adequate adsorbent has micropores and free functional groups in its chemical structure to realize physical or chemical interactions between the adsorbent and adsorbate, such as π–π and Van der Waals or ionic interactions. Physical characteristics such as porosity, surface area, and pore volume improve the adsorption capacity [13].

Removing toxic dyes from water has been a major goal of research for the last 10 years, and efforts have employed algae, agro-industrial wastes, and plant tissues (Table 1). The value of Q_m depends on the type of dye, the initial concentration, and the microstructure and chemical characteristics of the adsorbent. Some studies have reported the preparation and evaluation of biochar (carbon) from agro-industrial residues or plants, in many cases reporting a high adsorption rate (Table 1); however, the processes required to prepare biochar employ high temperatures and require the consumption of high levels of energy, making them less sustainable and unprofitable [16].

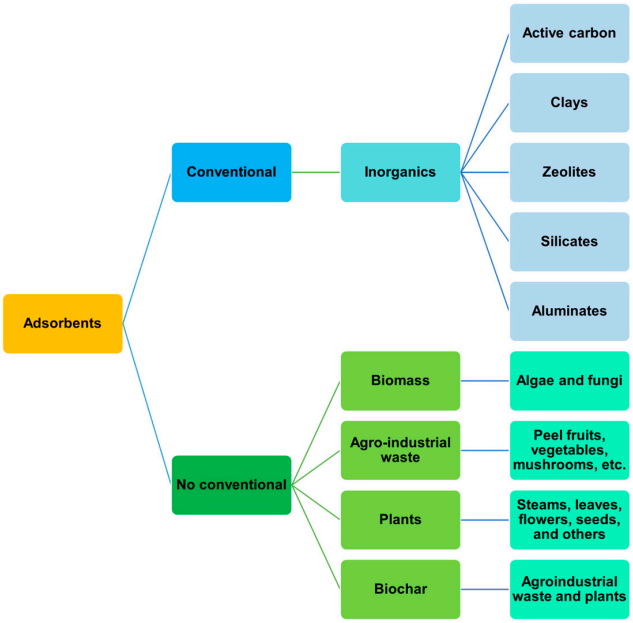

Figure 1. General classification of adsorbents.

Table 1. Non-conventional adsorbents from agro-industrial waste, algae, and plants used to remove azo dyes from water.

Dye	Adsorbent	Q_m (mg/g)	Reference
Acid Brown	Rice husk biochar [b]	10.4	[20]
Acid Orange 7	Extracted coffee residues biochar [b]	122.5	[21]
Alizarin Red S	Bamboo leaves biochar [c]	394.4	[22]
Brilliant Green		343.9	
Direct Orange 26	Sunflower husks [c]	11.0	[23]
Basic Red 2	*Leonurus cardiaca* leaves [c]	714.0	[24]
Methylene Blue	*Nizamuddinia zanardinii* [a]	142.1	[25]
	Gracilaria parvispora [a]	87.8	
	Ulva fasciata [a]	143.9	
	Sugarcane bagasse [b]	66.4	[26]
	Rice husk biochar [b]	11.8	[20]
	Shells Powders of Walnut and Peanut [b]	67.4 101.4	[27]
	Pine leaves [c]	140.8	[28]
Congo Red	Desiccated coconut waste [b]	0.07	[29]
Methyl Red	Raw corncob [b]	4.3	[30]
Methyl Orange	Lychee and longan pericarps [b]	349.4	[31]
	Raw corncob [b]	7.5	[30]
	Pine leaves [c]	136.9	[28]
Reactive Black 5	Eggshell membrane [b]	333.3	[32]
	Poplar sawdust [b]	0.8	[33]
Reactive Red 195	Eggshell membrane [b]	76.9	[32]
Reactive Red	Rice husk biochar [b]	11.8	[20]
Reactive Violet 5	Nannochloropsis [a]	115.0	[33]

[a] Algae, [b] Agro-industrial waste, [c] Plant.

Meanwhile, examples of using natural adsorbents to remove dyes from water without the requirement for expensive treatment include using *Leonurus cardiaca* leaves, which remove Basic Red 2 with a Q_m = 714.0 mg/g [24], and lychee (*Litchi chinensis*) and longan (*Dimocarpus longan*) pericarps, which remove Methyl Orange with a Q_m = 349.4 mg/g [31].

All of these dye removal studies have the same goal: to eliminate azo dyes from water. Moreover, it is necessary to study systems similar to real effluents because they frequently have high azo dye concentrations and contain mixtures of dyes. It is also necessary to evaluate their removal efficiency in scaled-up processes because applying non-conventional adsorbents on a large scale as treatment technologies with adequate adsorption and desorption capacity, durability, and reuse capacity leads to the design of better technologies [13]. However, the mechanisms by which natural and non-modified materials eliminate azo dyes from water are not widely reported [34]. In this context, non-conventional and non-modified *L. cylindrica* was studied regarding its physicochemical properties for its possible ability to remove azo dyes from water on a large scale via adsorption.

2. Materials and Methods

2.1. Non-Conventional and Low-Cost Adsorbent

L. cylindrica bulbs were collected from the town of Buenavista, Guerrero state, Mexico. They were transported to the laboratory to be cleaned (peel and seeds were eliminated) and then were cut into small pieces (1 cm^3), washed, and dried at 40 °C for 24 h (Figure 2).

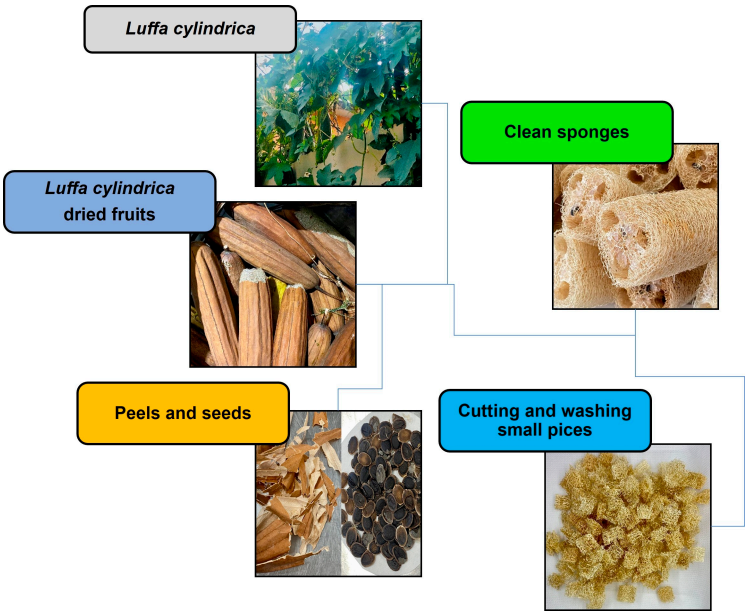

Figure 2. Preparation of non-conventional adsorbent.

2.2. Determination of Point Zero Charge

A total of 1.0 g of *L. cylindrica* was immersed for 48 h in 0.100 L of 0.01 M KNO_3 solution previously adjusted to different pH values from 3 to 11 using 0.1 M HCl and 0.1 M NaOH. Finally, the solution's pH was measured, and the difference in pH between the final and initial solution (Equation (1)) was plotted to determine the point zero charge as the intercept point on the abscissa axis, as described and suggested by Boudechiche [35] and Oun [36].

$$\Delta pH = pH_{Inicial} - pH_{final} \quad (1)$$

where the $\Delta pH = 0$ that is a pH_{pzc}.

2.3. Azo Dye Solution (Pollutant)

The azo dye (AD) mixture employed to develop all removal experiments was acquired at a local supermarket because it is extensively used as a textile dye at home to renew the color of blue jeans. The AD included nine different azo dyes (Disperse Blue 102 and 200; Direct Blue 71, 86, 151, and 201; Direct Yellow 50; Direct Red 23; and Direct Black 22) [37]. The AD was dissolved in distilled water (1000 mg/L), and different concentrations of AD, from 125 to 500 mg/L, were prepared. The solutions of AD were scanned using an ultraviolet–visible (UV-VIS) spectrophotometer from 320 to 700 nm, and one broad pick showed the maximum absorption at λ_{max} = 550 nm. This wavelength was used to measure the calibration curves in all adsorption experiments.

2.4. Adsorbent Dose Effect

L. cylindrica was studied at three doses (2.5, 5.0, and 10 g/L) using a solution of AD (250 mg/L) at 28 ± 2 °C and pH 7.0 with a contact time of 24 h. The residual AD was measured using spectrophotometric absorption (Agilent technology, Cary 100 UV–visible Spectrophotometer. Santa Clara, CA 95051, USA) and then the removal percentage was calculated using Equation (2).

$$R\% = \frac{C_0 - C_f}{C_0} * 100 \quad (2)$$

where C_0 and C_f are the initial and final concentrations, respectively.

2.5. Adsorption Studies

Adsorption experiments were realized in 2.0 L of the AD solution. Three concentrations (125, 250, and 500 mg/L) of the pollutant dye were used, and the adsorbent concentration was 10 g/L in all experiments. The conditions were 28 ± 2 °C and pH 7, and the residual AD was measured over 120 h with spectrophotometry at λ_{max} = 550 nm. The removal percentage was calculated using Equation (2), and the adsorption capacity in equilibrium was determined using Equation (3).

$$Q_e = \frac{(C_0 - C_e)V}{m} \quad (3)$$

where C_0 is the initial concentration, C_e is the concentration in the equilibrium, V is the volume, and m is the mass. All experiments were performed in triplicate, and the results were processed using Origin Pro-8 2018 Designer Software® to analyze and the statistical analysis of two factors was realized using Minitab 20 Statistical Software®.

2.6. Isotherm Models of Adsorption

Langmuir (Equation (4)), Freundlich (Equation (5)), and Temkin (Equation (6)) linearized isotherm models were employed to observe the adsorption of AD on *L. cylindrica* [31,38–40].

$$\frac{C_e}{Q_e} = \frac{1}{Q_m K_L} + \frac{1}{Q_m} C_e \quad (4)$$

where C_e (mg/L) is the concentration and Q_e (mg/g) is the adsorption capacity. Both are in equilibrium. Q_m(mg/g) is the maximum adsorption capacity, and K_L(L/mg) is Langmuir's constant.

$$log\ Q_e = \frac{1}{n} log C_e + log K_F \quad (5)$$

where K_f [(mg/g) (L/mg)1/n] is Freundlich's constant.

$$Q_e = B * Ln C_e + B * Ln K_T \quad (6)$$

where B (J/mol) is Temkin's constant, which is obtained by $B = {}^{RT}/_{b}$, where R is the universal gases constant (8.314 J/mol) and T is the temperature expressed in degrees Kelvin (°K). b is the adsorption energy variation and K_T is Temkin's equilibrium constant (L/mg).

2.7. Kinetic Models

The kinetic linearized pseudo-first-order (Equation (7)), pseudo-second-order (Equation (8)), Elovich (Equation (9)), and intraparticle diffusion (Equation (10)) models were utilized to analyze all experimental data [41–43].

$$Ln(Q_e - Q_t) = LnQ_e - k_1 t \tag{7}$$

$$\frac{t}{Q_t} = \frac{1}{k_2 {Q_e}^2} + \frac{1}{Q_e} t \tag{8}$$

$$Q_t = \frac{Ln\ (\alpha\beta)}{\beta} + \frac{1}{\beta} Ln\ t \tag{9}$$

$$Q_t = k_{id}\ t^{\frac{1}{2}} + C \tag{10}$$

where Q_t (mg/g) corresponds to the AD amount adsorbed at time t, k_1 is the adsorption rate (min^{-1}), t (min) is the time, k_2 is the second-order adsorption rate (g/mg min), k_{id} (mg/min g) is the intraparticle diffusion rate, and C is a constant.

2.8. Characterization of Luffa cylindrica

2.8.1. FTIR Spectroscopy

Fourier transformed infrared (FTIR) spectroscopy was measured on an Infrared Spectrophotometer FTIR-7600 Lambda Scientific Pty. Ltd (Edwardstown, Australia) equipped with an attenuated total reflectance (ATR) accessory. The samples were analyzed from 500 to 4000 cm^{-1} with 16 scans at 4 cm^{-1} resolution and a 1 cm^{-1} interval at room temperature.

2.8.2. FESEM Image of Natural Adsorbent

The morphology of the adsorbent was characterized using a field emission scanning electron microscope (FE-SEM), JSM-6390 LV JEOL.

2.9. Desorption Experiments

The determination of desorption pollutants and regenerating adsorbents was carried out using the thermal regeneration method with different solutions [44]. *L. cylindrica* (10 g/L) was immersed in 125 mL of AD solution (125, 250, and 500 mg/L) at pH 7.0 for 24 h (Figure 3). The *L. cylindrica* + AD material was dried at 80 °C for 1 h. The *L. cylindrica* + AD dried material (0.5 g) was immersed in 125 mL of H_2O, HCl (0.1 M), NaOH (0.1 M), and NaCl (0.1 M) for 4 h at 28 ± 2 °C. The desorption percentage (Equation (11)) and amount of AD desorbed (Equation (12)) were determined the following equations [45].

$$Desorption(\%) = \frac{C_D}{C_A} * 100 \tag{11}$$

$$Desorbed\ amount = \frac{C_{Ds}}{m} * V \tag{12}$$

where C_D (mg/g) is the concentration of AD desorbed, C_A (mg/g) is the concentration adsorbed (mg/g), C_{Ds} (mg/L) is the concentration of AD in the solution, m (g) is the mass of the adsorbent, and V (L) is the volume of the desorbing solution.

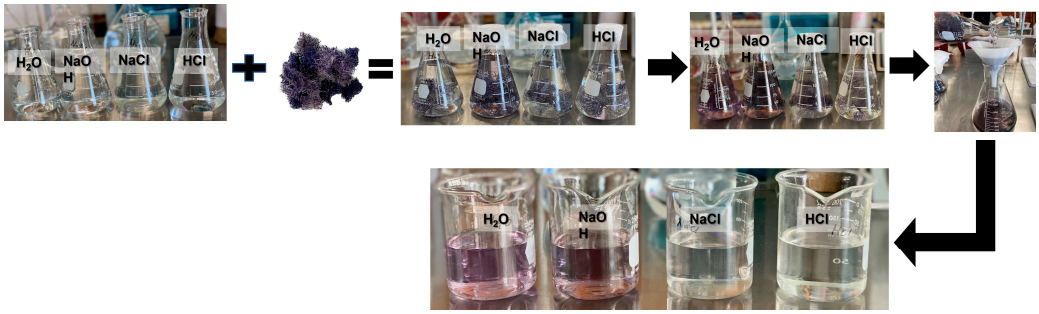

Figure 3. Desorption process of AD from *L. cylindrica*.

3. Results

3.1. Point Zero Charge Determination

Figure 4 shows the variation in the pH induced by *L. cylindrica* with respect to the initial pH solution. In acidic solutions (pH 3.0 to 5.0), the difference in pH (ΔpH) was negative. The pH_{pzc} to *L. cylindrica* was 6.5.

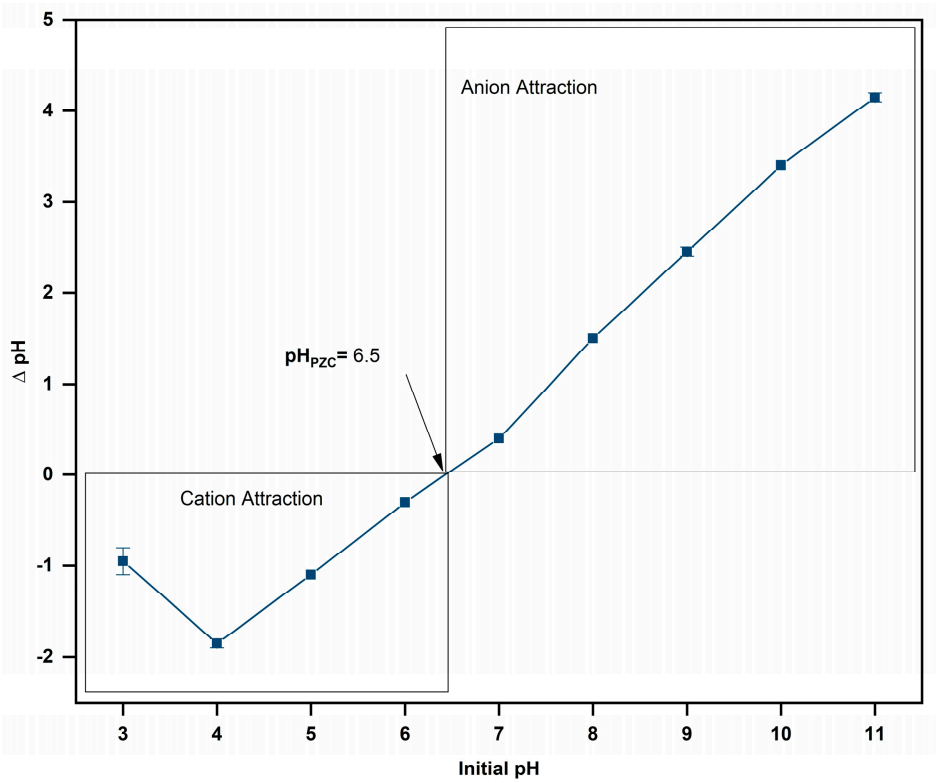

Figure 4. Determination of pH_{pzc} of *L. cylindrica*.

3.2. UV-VIS Spectroscopy of Azo Dye

The AD solution was analyzed using UV-VIS spectroscopy and showed a wide peak at 380 to 720 nm (Figure 5). The maximum peak observed for AD was observed at 550 nm. The calibration curve used in all experiments was realized at 550 nm to calculate the removal percentage and adsorption capacity (Q).

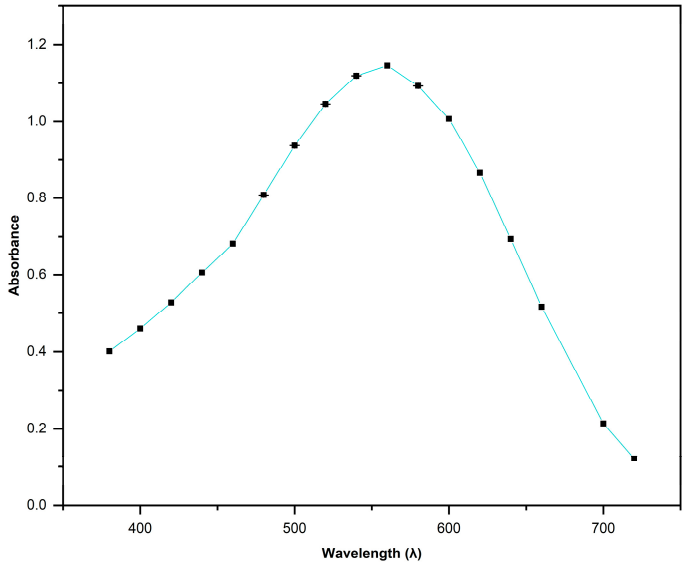

Figure 5. UV-VIS adsorption curve of AD [500 mg/L].

3.3. Effect of Adsorbent Doses

First, the adsorbent doses were determined using a single AD concentration (250 mg/L). Figure 6 shows the removal percentage produced by 2.5, 5.0, and 10.0 g/L of *L. cylindrica* as an adsorbent. The removal percentages after a contact time of 24 h were 20, 30, and 60%, respectively.

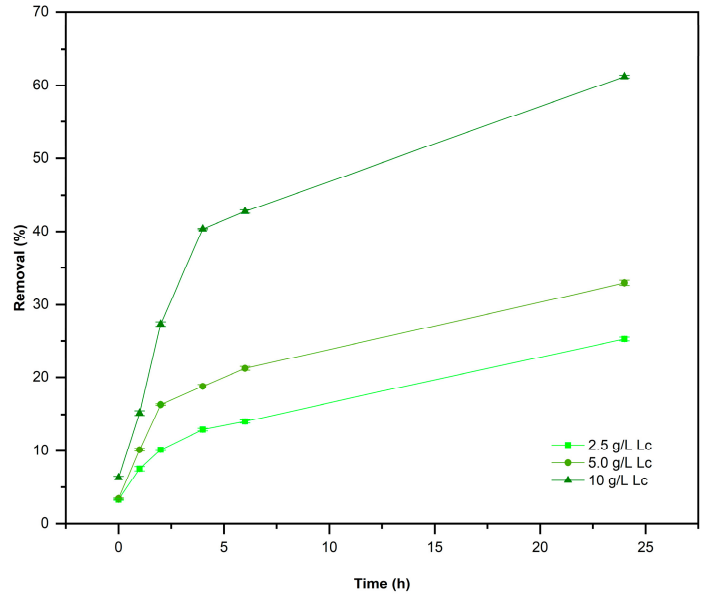

Figure 6. Removal percentage of AD [250 mg/L] using different doses of *L. cylindrica* (Lc). Conditions: 2.0 L, 28 ± 2 °C, and pH 7.0.

3.4. Adsorption Study

This study considered scaling up to remove three different concentrations of AD (125, 250, and 500 mg/L) and used 10.0 g/L of *L. cylindrica* for 5 days as the contact time. Figure 7 shows the results of adsorption study at the end of the resident time of 2 days (48 h), using the same doses of *L. cylindrica* [10 g/L] in all used AD concentrations. The maximum removal percentage was 62.07% for C_0 = 125 mg/L of AD, the removal rate reached 63.45% using AD at C_0 = 250 mg/L, and the removal rate was 58.61% in AD at C_0 = 500 mg/L. After 5 days the AD removal was stable without significant change. The adsorption capacity at

equilibrium (Q_e) occurred at 24 h as contact time (Figure 8) for all systems, as a significance of many free functional groups and the disposable contact sites [6]. The analysis of variance (p-value < 0.05) of two factors shows that contact time and concentration of AD have a significative influence on the Q_e and the removal of AD.

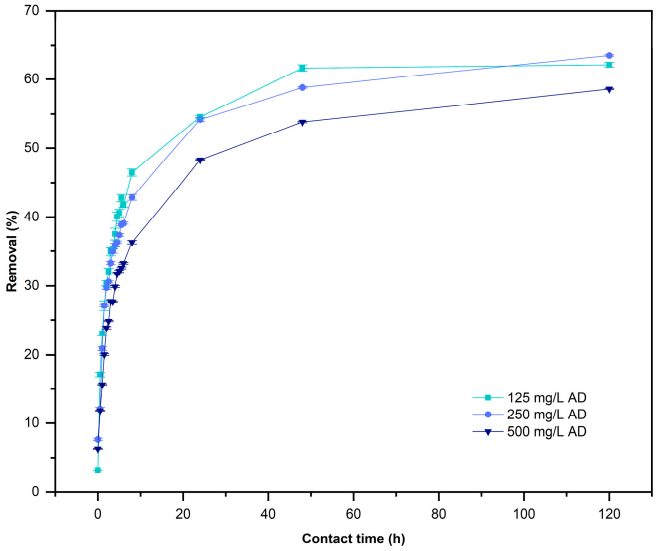

Figure 7. Removal of AD by *L. cylindrica*. (Conditions: 2.0 L working volume, 10 g/L of *L. cylindrica*, 28 ± 2 °C, and pH 7).

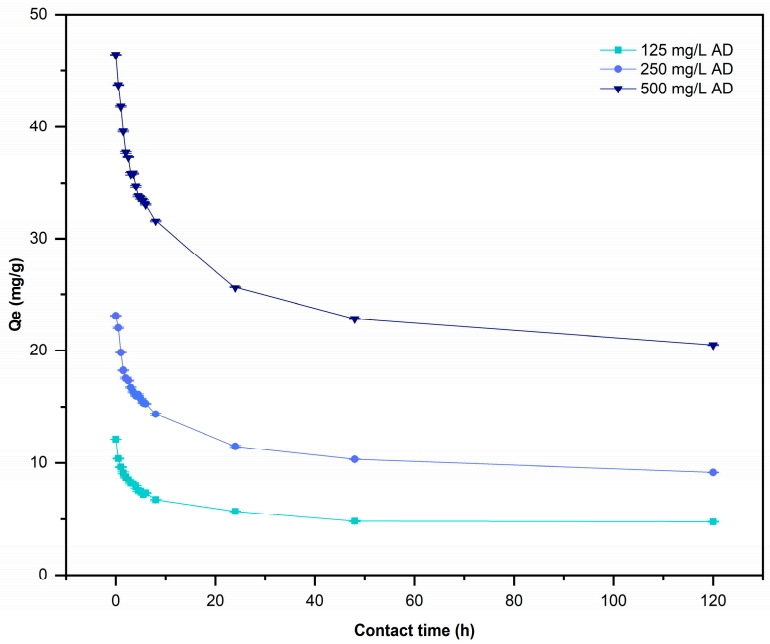

Figure 8. Effect of contact time on adsorption capacity of *L. cylindrica*. (Conditions: 2.0 L working volume, 28 ± 2 °C, and pH 7).

3.5. Isotherm of Adsorption

Langmuir, Freundlich, and Temkin isotherms were modeled for all adsorption experiments at a residence time of 24 h. The experimental data were adjusted to the Langmuir isotherm (Figure 9), and they did not fit the isotherm of the Freundlich and the Temkin models. Table 2 demonstrates that the maximum adsorption capacity (Q_m) of *L. cylindrica* obtained was 25.25 mg/g for C_0 = 500 mg/L of AD.

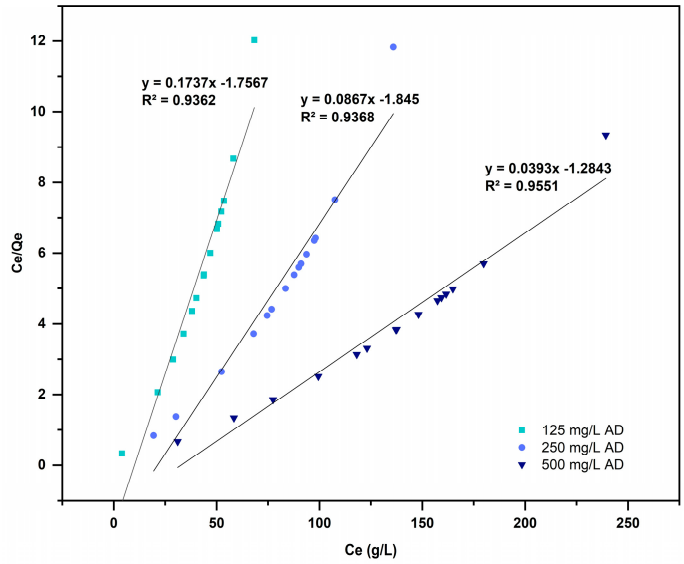

Figure 9. Langmuir isotherms for the adsorption of AD on *L. cylindrica*.

Table 2. Maximum adsorption capacity of AD using *L. cylindrica*.

AD C_0 [mg/L]	Q_m (mg/g)
125	5.76
250	11.51
500	25.45

3.6. Adsorption Kinetics

The kinetic models studied were the pseudo-first-order model, the pseudo-second-order model, and the intraparticle diffusion model of Weber and Morris, which are shown in Figure 10. According to the linear correlation, the thermodynamic model with the best fit was the pseudo-second-order model (Figure 10b). Table 3 shows the kinetic parameters obtained for the adsorption of AD on *L. cylindrica*.

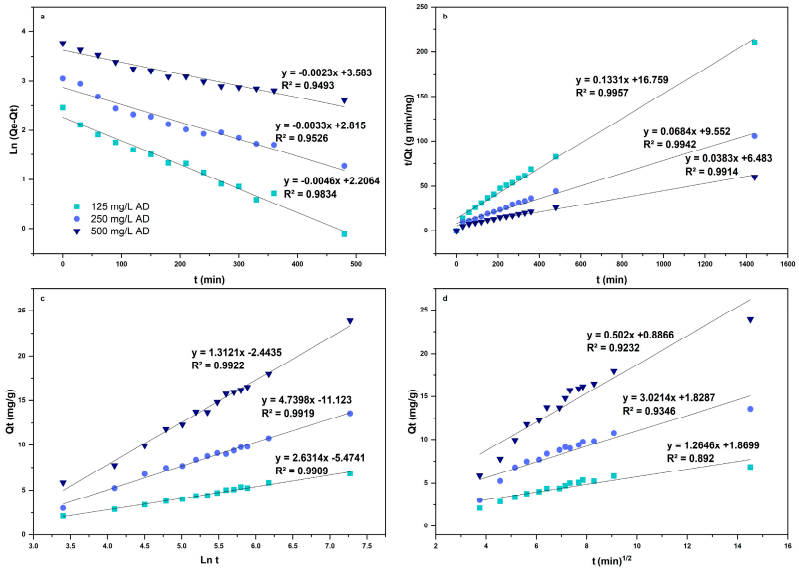

Figure 10. Kinetic models of the adsorption of AD on *L. cylindrica*. Pseudo-first-order model (**a**), pseudo-second-order model (**b**), Elovich model (**c**), and intraparticle diffusion model (**d**).

Table 3. Kinetic model parameters of AD adsorption on *L. cylindrica*.

AD [mg/L]		125	250	500
Pseudo-first-order model	R^2	0.983	0.953	0.949
	k_1 (min^{-1})	0.005	0.003	0.002
	Q_e, exp (mg/g)	6.705	14.325	31.566
	Q_e, cal (mg/g)	9.083	16.693	35.981
Pseudo-second-order model	R^2	0.997	0.994	0.991
	k_2 (g min/mg)	0.001	0.000	0.000
	Q_e, exp (mg/g)	6.705	14.325	31.566
	Q_e, cal (mg/g)	7.310	14.620	26.110
Intraparticle diffusion model	R^2	0.904	0.892	0.935
	K_{id}	0.485	1.265	3.021
	C	0.983	1.870	1.829
Elovich model	R^2	0.989	0.991	0.992
	β (g/mg)	0.780	0.380	0.211

3.7. Characterization of L. cylindrica Before and After Adsorption of AD

3.7.1. FTIR Analysis Spectroscopy

Figure 11 shows the FTIR spectra of *L. cylindrica* and AD before and after the adsorption experiments. The *L. cylindrica* FTIR spectrum (green line) shows the characteristic bands of lignin and cellulose fibers at 3282.82 cm^{-1}. This dominant peak is attributed to the stretching vibration of the -OH bond due to free hydroxyl groups. The peak at 2919.7 cm^{-1} is attributed to the -C-H bonds due to alkyl groups. The vibrations at 1627 and 1502 cm^{-1} are attributed to double bonds on aromatic carbons, as well as different types of carbohydrates such as cellulose, hemicellulose, and lignans [46,47].

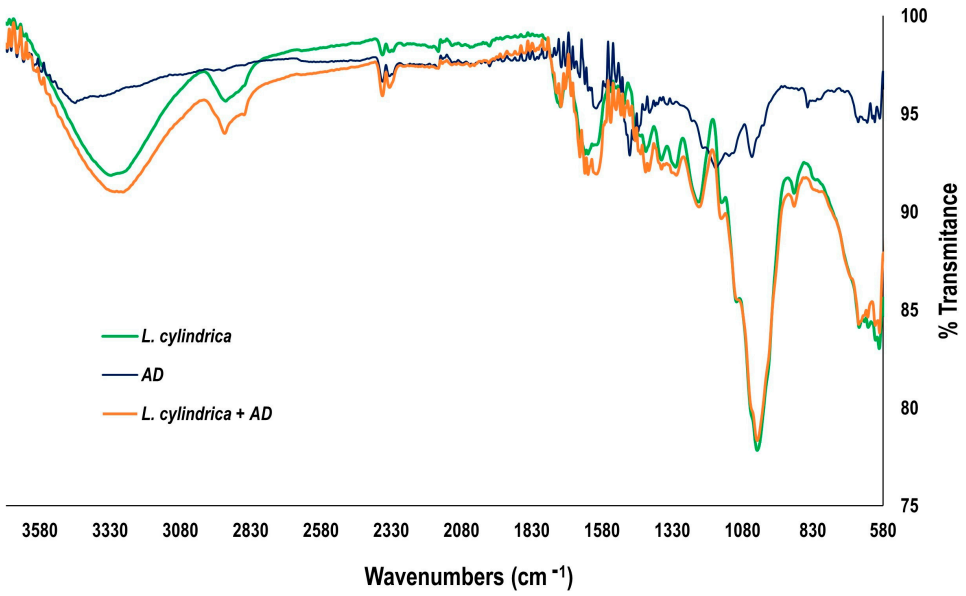

Figure 11. FTIR of *L. cylindrica* and AD before and after adsorption experiments.

The AD FTIR spectrum (blue line) shows the stretching vibration of the -OH bonds at 3453 cm^{-1}, which is a dominant peak. The two stretching vibrations at 2360 and 2331 cm^{-1} are attributed to $-CH_3$ and $-CH_2-$, respectively. The characteristic vibration at 1600 cm^{-1} is

attributed to the double carbon to carbon bonds (-C=C-) of aromatic rings. The important stretching vibration at 1481 cm^{-1} is attributed to an azo group (-N=N-), and at 1045 cm^{-1}, the vibration is assigned to the carbon–nitrogen bond (-C-N-), with both of them being dominant peaks. Another characteristic stretching vibration at 1174 cm^{-1} is attributed to the -S=O bonds. Finally, at 848 cm^{-1}, the stretching vibration is attributed to C-H aromatics and characteristic bonds in the chemical structure of diverse azo dyes [48,49].

The *L. cylindrica* + AD FTIR spectrum after the adsorption experiments (orange line) evidences the interactions between the functional groups of *L. cylindrica* and the AD molecules. The dominant peaks at 3328, 2894, and 1732–1482 cm^{-1} indicate the stronger interactions between the hydroxyl and carbonyl groups of *L. cylindrica* and the methylene hydrogens of the aromatic ring of the AD on the natural material surface.

3.7.2. FESEM Natural Adsorbent Analysis

L. cylindrica fibers were recorded by means of field emission scanning electron microscopy (FESEM) and analyzed regarding their microstructure and morphology before and after the adsorption experiments. Microimages are shown in Figure 12. Figure 12A corresponds to the *L. cylindrica* fibers before the experiment, and Figure 12B shows the *L. cylindrica* + AD after adsorption. At 10,000 and 50,000X, the morphological aspects are observed in both fibers. In *L. cylindrica* (Figure 12A), the surface looks smooth, rugose, and porous. These factors favor the adhesion of pollutants. In Figure 12B, the *L. cylindrica* + AD looks slightly softened due to the adhesion of AD [50,51].

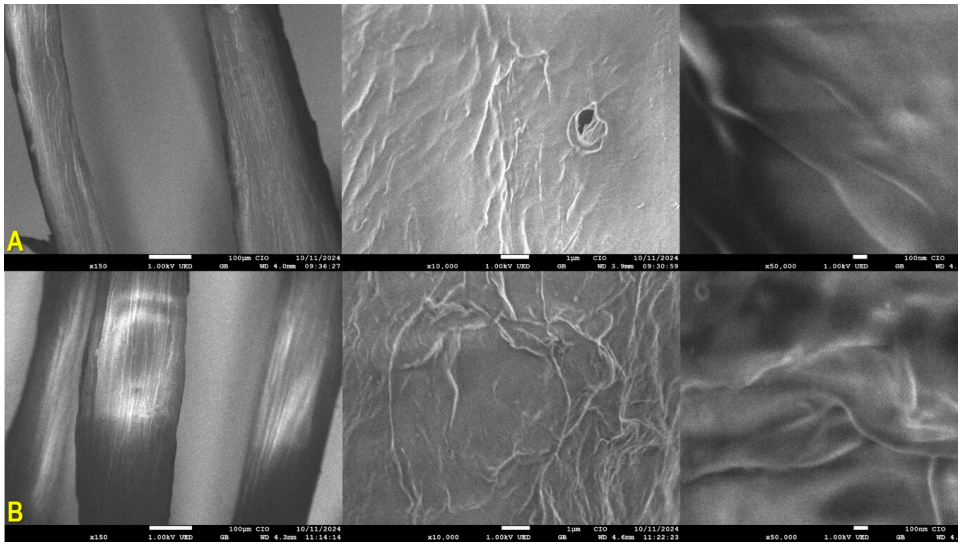

Figure 12. SEM images of *L. cylindrica* fibers before (**A**) and after (**B**) dye adsorption [0.500 mg/L at 24 h contact time].

3.8. Desorption Studies

Figure 13 shows the desorption efficiency of *L. cylindrica* at different pHs. A higher desorption of 95.8% was obtained in a basic pH (NaOH), while in a nearly neutral pH (distilled water), the desorption percentage was 63.3%. In contrast, in an acidic pH (HCl), the desorption was minimal, while in NaCl, it was null.

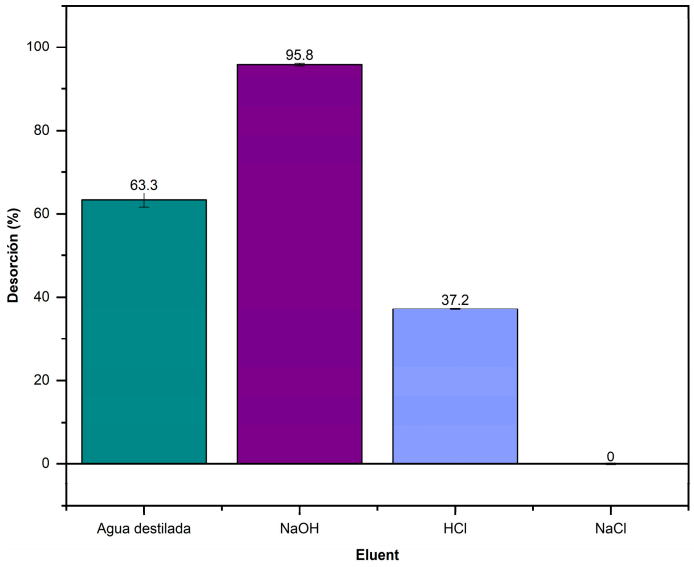

Figure 13. Desorption of AD on *L. cylindrica* in different pH solutions.

4. Discussion

The point zero charge (pH_{pzc}) represents the pH value in which the number of positive and negative charges between the internal and external surface of the adsorbent is zero [52]. pH_{pzc} is an important parameter to determine for lignocellulosic materials due to their amphoteric behavior. The pH affects adsorption processes because the functional groups can suffer ionization [53]. Theoretically, if the pH of the solution is close to 6.5 (pH_{pzc}), the surface of *L. cylindrica* is charged positively by protonation. It thus has a favorable tendency to attract and retain anionic molecules. However, if the solution's pH is below 6.5, the *L. cylindrica* surface is charged negatively by deprotonation and attracts and easily retains cationic molecules [53,54]. Some studies have reported that *L. cylindrica*-based adsorbents have a pH_{pzc} between 5.9 and 7.9 [54–56].

The maximum peak observed through UV-VIS spectroscopy for AD at 550 nm between 380 and 720 nm encompasses all individual absorbances that each azo dye contained. The individual absorbances reported for the single azo dyes included in the AD are 584 nm for Blue Azo dye 71 [57], 610–620 nm for Blue Azo dye 86 [58–60], 554 nm for Blue Azo dye 151 [57], 397 and 412 nm for Yellow Azo dye 50 [61,62], 550 nm for Red Azo dye 23 [63], and 481 nm for Black Azo dye 22 [64].

The removal percentages of AD by *L. cylindrica* after a contact time of 24 h were 20, 30, and 60%, respectively. A better removal percentage was obtained using 10.0 g/L of *L. cylindrica.* A similar effect was observed in small bath reactors, as previously reported by [37]. The concentration of azo dyes reported in wastewater varied from 100 to 500 mg/L [65] and *L. cylindrica* removed more than 50% of AD at 125, 250, and 500 mg/L until the system reached equilibrium. The adsorption capacity at equilibrium (Q_e) occurred after a contact time of 24 h (Figure 8) for the different systems as a result of there being many free functional groups and disposable contact sites [6]. The analysis of variance (p-value < 0.05) of the two factors shows that contact time and the concentration of AD have a significative influence on the adsorption capacity and removal of AD. After waiting for 5 days, the removal was stable without significant changes.

Some previous studies have evaluated the extraction of only one azo dye: for instance, Direct Blue 71 was removed at a rate of 21% using organic-rich compost [57]; Direct Blue 86 was removed using a rice-husk-based adsorbent, with a percentage removal of 40% using an initial dye concentration of 80 mg/L and a adsorbent dosage of 20 g/L [60]; and Direct Blue 151 was removed using compost, with 23 mg/g as the maximum sorption [57]. Using

20 g/L of cotton to remove Direct Yellow 50 at an initial concentration of 113.336 mg/L produced 20 mg/g as the maximum sorption [55]. Removing Direct Red 23 at an initial concentration of 150 mg/L using 10 g/L of activated carbon from *Cynara cardunculus* produced a maximum sorption of 14 mg/g [66]. The maximum adsorption capacity of eco-friendly spent mushroom waste was 15.46 mg/g for Direct Black 22 [67]. The removal percentages and maximum sorption values reported in these studies appear higher than our results. However, our AD contains nine azo dyes, and the natural adsorbent did not undergo previous chemical or thermal treatment. The Langmuir isotherm (Figure 9) describes the chemisorption behavior required to make Van der Waals interactions, hydrogen bonds, and π–π interactions [68,69]. The Q_m values reported for *L. cylindrica* using different dyes are between 9.6 mg/g and 49.46 mg/g, including Alphacide Blue [70], Trypan Blue [7], Methylene Blue [54], Reactive Yellow [71], and Malachite Green [72].

The Langmuir isotherm and the thermodynamic pseudo-second-order model produced the best linear correlation fits. Some reports have shown that in thermodynamic adsorption studies for azo dyes using *L. cylindrica*, better adjustment can be seen for the Langmuir isotherms and the pseudo-second-order model, for instance when using *L. cylindrica* sponge [70–72], *L. cylindrica* peel [54], and even a magnetic *L. cylindrica* sponge [7].

The interactions between the functional groups of *L. cylindrica* and the AD molecules are demonstrated on the *L. cylindrica* + AD FTIR spectrum after the adsorption experiments (Figure 11, orange line), and these results indicate that the adsorption of AD on the *L. cylindrica* surface occurs via physical adsorption following a Langmuir isotherm. Therefore, the changes in the intensity and displacement of some of the characteristic peaks showed that they were influenced by the electron environment and affected the bond vibration through formed interactions such as π–π interactions, van der Walls interactions, and hydrogen bonds [73–75].

The desorption results show that an alkaline environment favors the desorption of the AD onto *L. cylindrica* for its removal. A similar result was reported by Oliveira who mentioned a *L. cylindrica* desorption capacity of 72% for azo dye in a basic environment [71].

5. Conclusions

Luffa cylindrica, without treatment, removes between 58% and 63% of AD in a large-scale solution with concentrations of 125 mg/L and 500 mg/L, respectively. The maximum adsorption capacity was 25.45 mg/g. The analysis of variance (p-value < 0.05) shows that the contact time and concentration of AD have a significative influence on the adsorption capacity and removal of AD. *L. cylindrica* desorbed 95.8% of the AD in 0.1 M NaOH. This study examined the environmentally friendly removal of a nonary mixture of azo dyes from water using a natural, non-conventional, and low-cost adsorbent. This study shows that *L. cylindrica* removes diverse azo dyes from water on a large scale, resulting in an promising, environmentally friendly alternative to reducing organic material from wastewater. *L cylindrica* could therefore be incorporated in coupled wastewater treatments.

Author Contributions: Conceptualization, M.G.V.-C.; methodology, M.G.A.-F.; validation M.G.V.-C., R.J.R., A.R.-T., A.R., Á.T.-I., D.M.A.-A. and G.I.B.-L., Formal analysis M.G.V.-C., M.R., R.J.R., D.M.A.-A. and G.I.B.-L.; writing—original draft preparation M.G.A.-F. and M.G.V.-C.; writing—review and editing M.G.V.-C. and R.J.R. All authors have read and agreed to the published version of the manuscript.

Funding: This research received no external funding.

Institutional Review Board Statement: Not applicable.

Informed Consent Statement: Not applicable.

Data Availability Statement: The original contributions presented in this study are included in the article. Further inquiries can be directed to the corresponding author.

Acknowledgments: The authors would like to sincerely thank the Consejo Nacional de Humanidades, Ciencia y Tecnología (CONAHCYT) for the fellowship and would also like to thank sincerely the Laboratory of Bioactive Phytochemical Products, Faculty of Engineering and Chemical Sciences, Autonomous University of Morelos State, for the hosting of experiments and skilled laboratory support.

Conflicts of Interest: The authors declare no conflicts of interest.

Abbreviations

The following abbreviations are used in this manuscript:

AD	Azo dye
BOD	Biological oxygen demand
COD	Chemical oxygen demand
TSS	Total suspended solids
NaOH	Sodium hydroxide
HCl	Hydrogen chloride
KNO_3	Potassium nitrate
pH	Hydrogen potential
M	Molarity
UV-VIS	Ultraviolet–visible
FTIR	Fourier transformed infrared
FE-SEM	Field emission scanning electron microscope
pH_{pzc}	Point charge zero
C_0	Initial concentration
C_e	Equilibrium concentration
Q_m	Maximum adsorption capacity

References

1. Münzel, T.; Hahad, O.; Daiber, A.; Landrigan, P.J. Soil and water pollution and human health: What should cardiologists worry about? *Cardiovasc. Res.* **2023**, *119*, 440–449. [CrossRef] [PubMed]
2. Babuji, P.; Thirumalaisamy, S.; Duraisamy, K.; Periyasamy, G. Human health risks due to exposure to water pollution: A review. *Water* **2023**, *15*, 2532. [CrossRef]
3. Mishra, R.K. Freshwater availability and its global challenge. *BJMAS* **2023**, *4*, 1–78. [CrossRef]
4. Riffat, R.; Husnain, T. *Fundamentals of Wastewater Treatment and Engineering*, 2nd ed.; CRC Press: Abingdon, UK, 2022. [CrossRef]
5. Kishor, R.; Purchase, D.; Saratale, G.D.; Saratale, R.G.; Romanholo Ferreira, L.F.; Bilal, M.; Chandra, R.; Bharagava, R.N. Ecotoxicological and health concerns of persistent coloring pollutants of textile industry wastewater and treatment approaches for environmental safety. *J. Environ. Chem. Eng.* **2021**, *9*, 105012. [CrossRef]
6. Khadir, A.; Negarestani, M.; Kheradmand, A.; Azad, A.; Sillanpää, M. The Utilization of Biomaterials for Water Purification: Dyes, Heavy Metals, and Pharmaceuticals. In *Novel Materials for Dye-Containing Wastewater Treatment. Sustainable Textiles: Production, Processing, Manufacturing & Chemistry*; Muthu, S.S., Khadir, A., Eds.; Springer: Singapore, 2021; pp. 27–58. [CrossRef]
7. Nadaroglu, H.; Cicek, S.; Onem, H.; Gungor, A.A. The Investigation of Removing Direct Blue 15 Dye from Wastewater Using Magnetic Luffa sponge NPs. In *Iron Ores and Iron Oxide Materials*; Shatokha, V., Ed.; InTech: London, UK, 2018. [CrossRef]
8. Berradi, M.; Hsissou, R.; Khudhair, M.; Assouag, M.; Cherkaoui, O.; El Bachiri, A.; El Harfi, A. Textile finishing dyes and their impact on aquatic environs. *Heliyon* **2019**, *5*, e02711. [CrossRef]
9. Rawat, D.; Mishra, V.; Sharma, R.S. Detoxification of azo dyes in the context of environmental processes. *Chemosphere* **2016**, *155*, 591–605. [CrossRef]
10. Srinivasan, A.; Viraraghavan, T. Decolorization of dye wastewaters by biosorbents: A review. *J. Environ. Manag.* **2010**, *91*, 1915–1929. [CrossRef]
11. Tkaczyk-Wlizło, A.; Mitrowska, K.; Błądek, T. Quantification of twenty pharmacologically active dyes in water samples using UPLC-MS/MS. *Heliyon* **2022**, *8*, e09331. [CrossRef] [PubMed]

12. Barrios-Ziolo, L.F.; Gaviria-Restrepo, L.F.; Agudelo, E.A.; Cardona-Gallo, S.A. Technologies for the removal of dyes and pigments present in wastewater. A review. *Dyna* **2015**, *82*, 118–126. [CrossRef]
13. Li, W.; Mu, B.; Yang, Y. Feasibility of industrial-scale treatment of dye wastewater via bio-adsorption technology. *Bioresour. Technol.* **2019**, *277*, 157–170. [CrossRef]
14. Rashid, R.; Shafiq, I.; Akhter, P.; Iqbal, M.J.; Hussain, M. A state-of-the-art review on wastewater treatment techniques: The effectiveness of adsorption method. *Environ. Sci. Pollut. Res.* **2021**, *28*, 9050–9066. [CrossRef] [PubMed]
15. Sonune, A.; Ghate, R. Developments in wastewater treatment methods. *Desalination* **2004**, *167*, 55–63. [CrossRef]
16. Muthu, S.S.; Khadir, A. *Novel Materials for Dye-Containing Wastewater Treatment*; Springer: Singapore, 2021. [CrossRef]
17. Natrayan, L.; Niveditha, V.R.; Nadh, V.S.; Srinivas, C.; Dhanraj, J.A.; Saravanan, A. Application of response surface and artificial neural network optimization approaches for exploring methylene blue adsorption using luffa fiber treated with sodium chlorite. *J. Water Proc. Eng.* **2024**, *58*, 104778. [CrossRef]
18. Valladares-Cisneros, M.G.; Valerio-Cárdenas, C.; de la Cruz-Burelo, P.; Melgoza-Alemán, R.M. Adsorbentes no-convencionales, alternativas sustentables para el tratamiento de aguas residuales. *RIUM* **2017**, *16*, 55–73. [CrossRef]
19. Torres, E. Biosorption: A review of the latest advances. *Processes* **2020**, *8*, 1584. [CrossRef]
20. Arivumani, V.; Singh, V.; Geetha, C.; Senthilkumar, C. Activated rice husk biochar for azo dye removal: Batch adsorption, kinetics, and thermodynamic studies. *Glob. NEST* **2024**, *26*, 05498. [CrossRef]
21. Jung, K.-W.; Choi, B.H.; Hwang, M.-J.; Choi, J.-W.; Lee, S.-H.; Chang, J.-S.; Ahn, K.-H. Adsorptive removal of anionic azo dye from aqueous solution using activated carbon derived from extracted coffee residues. *J. Clean. Prod.* **2017**, *166*, 360–368. [CrossRef]
22. Tran, T.T.H.; Vu, N.T.; Pham, T.N.; Nguyen, X.T. Ability to Remove Azo Dye from Textile Dyeing Wastewaters of Carbonaceous Materials Produced from Bamboo Leaves. In *Novel Materials for Dye-containing Wastewater Treatment. Sustainable Textiles: Production, Processing, Manufacturing & Chemistry*; Muthu, S.S., Khadir, A., Eds.; Springer: Singapore, 2021; pp. 185–208. [CrossRef]
23. Tomczak, E.; Tosik, P. Waste plant material as a potential adsorbent of a selected azo dye. *Chem. Process Eng.* **2017**, *38*, 283–294. [CrossRef]
24. Akdemir, M.; Isik, B.; Cakar, F.; Cankurtaran, O. High-performing natural materials (*Leonurus cardiaca*): Dye biosorption studies and statistical analysis. *Biomass Convers. Biorefin.* **2023**, *13*, 14281–14299. [CrossRef]
25. Daneshvar, E.; Vazirzadeh, A.; Niazi, A.; Sillanpää, M.; Bhatnagar, A. A Comparative study of methylene blue biosorption using different modified brown, red, and green macroalgae–Effect of pretreatment. *Chem. Eng. J.* **2017**, *307*, 435–446. [CrossRef]
26. Fathana, H.; Rahmi; Adlim, M.; Lubis, S.; Iqhrammullah, M. Sugarcane bagasse-derived cellulose as an eco-friendly adsorbent for azo dye removal. *IIETA* **2023**, *18*, 11–20. [CrossRef]
27. Benjelloun, M.; Miyah, Y.; Bouslamti, R.; Nahali, L.; Mejbar, F.; Lairini, S. The fast-efficient adsorption process of the toxic dye onto shell powders of walnut and peanut: Experiments, equilibrium, thermodynamic, and regeneration studies. *Chem. Afr.* **2022**, *5*, 375–393. [CrossRef]
28. Huynh, P.T.; Nguyen, D.K.; Duong, B.N.; Nguyen, P.H.; Dinh, V.P. Methylene Orange and Methyl Blue Adsorption Behavior on Pine Leaves Biomass (*Pinus kesiya*). *Res. Sq.* **2023**, *1*, 1–20. [CrossRef]
29. Abdul Rahim, A.R.; Mohsin, H.M.; Chin, K.B.; Johari, K.; Saman, N. Promising low-cost adsorbent from desiccated coconut waste for removal of Congo red dye from aqueous solution. *Water Air Soil Poll.* **2021**, *232*, 357. [CrossRef]
30. Salih, S.J.; Kareem, A.S.; Anwer, S.S. Adsorption of anionic dyes from textile wastewater utilizing raw corncob. *Heliyon* **2022**, *8*, e10092. [CrossRef]
31. Ma, J.; Hou, L.; Li, P.; Zhang, S.; Zheng, X. Modified fruit pericarp as an effective biosorbent for removing azo dye from aqueous solution: Study of adsorption properties and mechanisms. *Environ. Eng. Res.* **2022**, *27*, 200634. [CrossRef]
32. Dinçer, A.; Sevildik, M.; Aydemir, T. Optimization, isotherm, and kinetics studies of azo dye adsorption on eggshell membrane. *Int. J. Chem. Technol.* **2019**, *3*, 52–60. [CrossRef]
33. Hosseinzehi, M.; Khatebasreh, M.; Dalvand, A. Modeling of Reactive Black 5 azo dye adsorption from aqueous solution on activated carbon prepared from poplar sawdust using response surface methodology. *Int. J. Environ. Anal. Chem.* **2022**, *102*, 6970–6987. [CrossRef]
34. Caicho-Caranqui, J.; Vivanco, G.; Egas, D.A.; Cristina Chuya-Sumba, C.; Guerrero, V.H.; Ramirez-Cando, L.; Reinoso, C.; De Sousa, F.B.; Leon, M.; Ochoa-Herrera, V.; et al. Non-modified cellulose fibers for toxic heavy metal adsorption from water. *Adsorption* **2025**, *31*, 18. [CrossRef]
35. Boudechiche, N.; Mokaddem, H.; Sadaoui, Z.; Trari, M. Biosorption of cationic dye from aqueous solutions onto lignocellulosic biomass (*Luffa cylindrica*): Characterization, equilibrium, kinetic and thermodynamic studies. *Int. J. Ind. Chem.* **2016**, *7*, 167–180. [CrossRef]
36. Oun, A.A.; Kamal, K.H.; Farroh, K.; Ali, E.F.; Hassan, M.A. Development of fast and high-efficiency sponge-gourd fibers (*Luffa cylindrica*)/hydroxyapatite composites for removal of lead and methylene blue. *Arab. J. Chem.* **2021**, *14*, 103281. [CrossRef]

37. Aranda-Figueroa, M.; Rodríguez-Torres, A.; Rodríguez, A.; Bolio-López, G.; Salinas-Sánchez, D.; Arias-Atayde, D.; Romero, R.J.; Valladares-Cisneros, M.G. Removal of Azo Dyes from Water Using Natural Luffa cylindrica as a Non-Conventional Adsorbent. *Molecules* **2024**, *29*, 1954. [CrossRef] [PubMed]
38. Faraj, M.; Erhayem, M. Langmuir, Freundlich, Temkin, and Dubinin–Radushkevich isotherm studies of equilibrium sorption of Methylene Blue from Aqueous Solution onto Mulberry tree (*Morus nigra* L) roots powder. *JOPAS* **2018**, *17*, 100–107. [CrossRef]
39. Faraj, M.; Erhayem, M.; Mohamed, R. Kinetics and Thermodynamic Study for Adsorption of Methylene Blue onto Mulberry Tree (*Morus nigra* L) Roots Powder. *JOPAS* **2019**, *18*, 1–6. [CrossRef]
40. Chen, X. Modeling of experimental adsorption isotherm data. *Information* **2015**, *6*, 14–22. [CrossRef]
41. Emene, A.U.; Edyvean, R.; Akpan, U.G. Light-assisted adsorption of methylene blue onto *Luffa cylindrica*. *Desalin. Water Treat.* **2021**, *216*, 379–388. [CrossRef]
42. Henini, G.; Laidani, Y.; Souahi, F. Study of the kinetics and thermodynamics of adsorption of Red Bemacid on the cords of *Luffa cylindrica*. *Desalin. Water Treat.* **2016**, *57*, 3741–3749. [CrossRef]
43. Tejada-Tovar, C.; Villabona-Ortíz, Á.; Gonzalez-Delgado, Á.D. Adsorption of azo-anionic dyes in a solution using modified coconut (*Cocos nucifera*) mesocarp: Kinetic and equilibrium study. *Water* **2021**, *13*, 1382. [CrossRef]
44. Zanella, O.; Tessaro, I.C.; Féris, L.A. Desorption-and decomposition-based techniques for the regeneration of activated carbon. *Chem. Eng. Technol.* **2014**, *37*, 1447–1459. [CrossRef]
45. Patel, H. Review on solvent desorption study from the exhausted adsorbent. *J. Saudi Chem. Soc.* **2021**, *25*, 101302. [CrossRef]
46. Hong, T.; Yin, J.Y.; Nie, S.P.; Xie, M.Y. Applications of infrared spectroscopy in polysaccharide structural analysis: Progress, challenge, and perspective. *Food Chem. X* **2021**, *12*, 100168. [CrossRef] [PubMed]
47. Javier-Astete, R.; Jimenez-Davalos, J.; Zolla, G. Determination of hemicellulose, cellulose, holocellulose and lignin content using FTIR in *Calycophyllum spruceanum* (Benth.) K. Schum. and *Guazuma crinita* Lam. *PLoS ONE* **2021**, *16*, e0256559. [CrossRef] [PubMed]
48. Mbarek, W.B.; Daza, J.; Escoda, L.; Fiol, N.; Pineda, E.; Khitouni, M.; Suñol, J.J. Removal of reactive black 5 azo Dye from aqueous solutions by a combination of reduction and natural adsorbents processes. *Metals* **2023**, *13*, 474. [CrossRef]
49. Jawad, A.H.; Ngoh, Y.S.; Radzun, K.A. Utilization of watermelon (*Citrullus lanatus*) rinds as a natural low-cost biosorbent for adsorption of methylene blue: Kinetic, equilibrium and thermodynamic studies. *J. Taibah Univ. Sci.* **2018**, *12*, 371–381. [CrossRef]
50. Tolkou, A.K.; Tsoutsa, E.K.; Katsoyiannis, I.A.; Kyzas, G.Z. Simultaneous removal of anionic and cationic dyes on quaternary mixtures by adsorption onto banana, orange, and pomegranate peels. *Colloids Surf. A* **2024**, *685*, 133176. [CrossRef]
51. Rauf, A.; Mahmud, T.; Ashraf, C.M.; Rehman, R. Sorptive Removal of Alizarin Yellow-R Dye from the Water Using Fibers of *Luffa cylindrica* Sponge. *Int. J. Environ. Sustain.* **2016**, *12*, 31. [CrossRef]
52. Villa, F.A. Determinación del punto de carga cero y punto isoeléctrico de dos residuos agrícolas y su aplicación en la remoción de colorantes. *RIAA* **2013**, *4*, 27–36. [CrossRef]
53. Ye, C.; Hu, N.; Wang, Z. Experimental investigation of Luffa cylindrica as a natural sorbent material for the removal of a cationic surfactant. *J. Taiwan Inst. Chem. Eng.* **2013**, *44*, 74–80. [CrossRef]
54. Ng, H.W.; Lee, L.Y.; Chan, W.L.; Gan, S.; Chemmangattuvalappil, N. Luffa acutangula peel as an effective natural biosorbent for malachite green removal in aqueous media: Equilibrium, kinetic and thermodynamic investigations. *Desalin. Water Treat.* **2016**, *57*, 7302–7311. [CrossRef]
55. Anastopoulos, I.; Pashalidis, I. The application of oxidized carbon derived from *Luffa cylindrica* for caffeine removal. Equilibrium, thermodynamic, kinetic and mechanistic analysis. *J. Mol. Liq.* **2019**, *296*, 112078. [CrossRef]
56. Mashkoor, F.; Nasar, A. Preparation, characterization, and adsorption studies of the chemically modified *Luffa aegyptica* peel as a potential adsorbent for the removal of malachite green from aqueous solution. *J. Mol. Liq.* **2019**, *274*, 317–327. [CrossRef]
57. Al-Zawahreh, K.; Barral, M.T.; Al-Degs, Y.; Paradelo, R. Comparison of the sorption capacity of basic, acid, direct, and reactive dyes by compost in batch conditions. *J. Environ. Manag.* **2021**, *294*, 113005. [CrossRef]
58. Shoaib, A.G.; El Nemr, A.; Ramadan, M.S.; Masoud, M.S.; El Sikaily, A. Composite fabrication and characterization of crosslinked polyaniline/Pterocladia capillacea-activated carbon for adsorption of direct blue-86 dye from water. *Polym. Bull.* **2023**, *80*, 10393–10428. [CrossRef]
59. Kumar, D.; Gupta, S.K. Green synthesis of novel biochar from Abelmoschus esculentus seeds for direct blue 86 dye removal: Characterization, RSM optimization, isotherms, kinetics, and fixed bed column studies. *Environ. Pollut.* **2023**, *337*, 122559. [CrossRef] [PubMed]
60. Zua, M.Z.; Mustafa, M.R.; Abd Manan, T.S.; Ibrahim, N. Direct Blue 86 Textile Dye Removal from Aqueous Solution Using Rice Husk-based Adsorbent. *ASEAN J. Sci. Technol. Dev.* **2023**, *40*, 44–248. [CrossRef]
61. Mahmoud, A.S. Effect of nano bentonite on direct yellow 50 dye removal; Adsorption isotherm, kinetic analysis, and thermodynamic behavior. *Prog. React. Kinet. Mech.* **2022**, *47*, 14686783221090377. [CrossRef]

62. Ismail, L.F.; Sallam, H.B.; Farha, S.A.; Gamal, A.M.; Mahmoud, G.E. Adsorption behaviour of direct yellow 50 onto cotton fiber: Equilibrium, kinetic and thermodynamic profile. *Spectrochim. Acta A Mol. Biomol. Spectrosc.* **2014**, *131*, 657–666. [CrossRef] [PubMed]
63. Konicki, W.; Pełech, I.; Mijowska, E.; Jasińska, I. Adsorption of anionic dye Direct Red 23 onto magnetic multi-walled carbon nanotubes-Fe_3C nanocomposite: Kinetics, equilibrium, and thermodynamics. *Chem. Eng. J.* **2012**, *210*, 87–95. [CrossRef]
64. Alexandre, J.I.D.S.; Santos Neto, S.M.D.; Coutinho, A.P.; Melo, T.D.A.T.D.; Gonçalves, E.A.P.; Gondim, M.V.S.; Antonino, A.C.D.; Rabelo, A.E.C.D.G.D.C.; Oliveira, A.L.D. Sorption of the Direct Black 22 dye in alluvial soil. *Rev. Amb. Água* **2020**, *15*, e2483. [CrossRef]
65. Zaruma, P.; Proal, J.; Hernández, I.C.; Salas, H.I. Los colorantes textiles industriales y tratamientos óptimos de sus efluentes de agua residual: Una breve revisión. *Revista de la Facultad de Ciencias Químicas* **2018**, *19*, 38–47.
66. El Nemr, A.; El Sadaawy, M.M.; Khaled, A.; El Sikaily, A. Adsorption of the anionic dye Direct Red 23 onto new activated carbons developed from *Cynara cardunculus*: Kinetics, equilibrium and thermodynamics. *Blue Biotechnol. J.* **2014**, *3*, 121–142.
67. Alhujaily, A.; Yu, H.; Zhang, X.; Ma, F. Adsorptive removal of anionic dyes from aqueous solutions using spent mushroom waste. *Appl. Water Sci.* **2020**, *10*, 1–12. [CrossRef]
68. Piccin, J.S.; Cadaval, T.R.S.A.; De Pinto, L.A.A.; Dotto, G.L. Adsorption isotherms in liquid phase: Experimental, modeling, and interpretations. In *Adsorption Processes for Water Treatment and Purification*; Bonilla-Petriciolet, A., Mendoza-Castillo, D.I., Reynel-Ávila, H.E., Eds.; Springer: Berlin/Heidelberg, Germany, 2017; pp. 19–51. [CrossRef]
69. El-Hendawy, A.N.A.; Alexander, A.J.; Andrews, R.J.; Forrest, G. Effects of activation schemes on porous, surface and thermal properties of activated carbons prepared from cotton stalks. *JAAP* **2008**, *82*, 272–278. [CrossRef]
70. Kesraoui, A.; Moussa, A.; Ali, G.B.; Seffen, M. Biosorption of alpacide blue from aqueous solution by lignocellulosic biomass: *Luffa cylindrica* fibers. *Environ. Sci. Pollut. Res.* **2016**, *23*, 15832–15840. [CrossRef] [PubMed]
71. Oliveira, E.; Montanher, S.; Rollemberg, M. Removal of textile dyes by sorption on low-cost sorbents. A case study: Sorption of reactive dyes onto *Luffa cylindrica*. *Desalin. Water Treat.* **2011**, *25*, 54–64. [CrossRef]
72. Altınışık, A.; Gür, E.; Seki, Y. A natural sorbent, *Luffa cylindrica* for the removal of a model basic dye. *J. Hazard. Mater.* **2010**, *179*, 658–664. [CrossRef]
73. Cao, S.; Zhu, R.; Wu, D.; Su, H.; Liu, Z.; Chen, Z. How hydrogen bonding and π–π interactions synergistically facilitate mephedrone adsorption by bio-sorbent: An in-depth microscopic scale interpretation. *Environ. Pollut.* **2024**, *342*, 123044. [CrossRef]
74. Liu, Y.; Cao, S.; Xi, C.; Su, H.; Chen, Z. A new nanocomposite assembled with metal organic framework and magnetic biochar derived from pomelo peels: A highly efficient adsorbent for ketamine in wastewater. *J. Environ. Chem. Eng.* **2021**, *9*, 106207. [CrossRef]
75. Chen, T.; Li, M.; Liu, J. π–π stacking interaction: A nondestructive and facile means in material engineering for bioapplications. *Cryst. Growth Des.* **2018**, *18*, 2765–2783. [CrossRef]